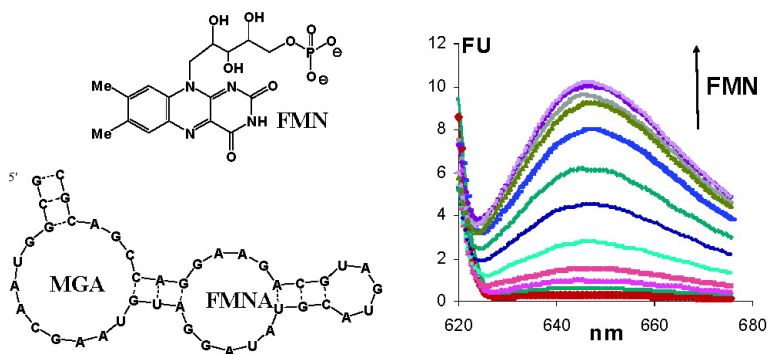


## Modular Aptameric Sensors

Milan N. Stojanovic, and Dmitry M. Kolpashchikov

*J. Am. Chem. Soc.*, **2004**, 126 (30), 9266-9270 • DOI: 10.1021/ja032013t • Publication Date (Web): 08 July 2004

Downloaded from <http://pubs.acs.org> on April 1, 2009



### More About This Article

Additional resources and features associated with this article are available within the HTML version:

- Supporting Information
- Links to the 10 articles that cite this article, as of the time of this article download
- Access to high resolution figures
- Links to articles and content related to this article
- Copyright permission to reproduce figures and/or text from this article

[View the Full Text HTML](#)

## Modular Aptameric Sensors

Milan N. Stojanovic\* and Dmitry M. Kolpashchikov

*Contribution from the Division of Experimental Therapeutics, Department of Medicine, Columbia University, New York, New York 10032*

Received December 31, 2003; E-mail: mns18@columbia.edu

**Abstract:** We report the first examples of modular aptameric sensors, which transduce recognition events into fluorescence changes through allosteric regulation of noncovalent interactions with a fluorophore. These sensors consist of: (a) a reporting domain, which signals the binding event of an analyte through binding to a fluorophore; (b) a recognition domain, which binds the analyte; and (c) a communication module, which serves as a conduit between recognition and signaling domains. We tested recognition regions specific for **ATP**, **FMN**, and theophylline in combinations with malachite green binding aptamer as a signaling domain. In each case, we were able to obtain a functional sensor capable of responding to an increase in analyte concentration with an increase in fluorescence. Similar constructs that consist only of natural RNA could be expressed in cells and used as sensors for intracellular imaging.

## Introduction

Several groups,<sup>1</sup> including ours,<sup>2</sup> recently reported successful approaches to fluorescent aptameric sensors for small molecules and proteins. However, none of these approaches are readily adaptable to intracellular imaging applications. In particular, the reported methods depend on labeled or unnatural DNA or RNA molecules. Therefore, the sensors require exogenous delivery, in contrast to fluorescent proteins that can be expressed in cells.<sup>3</sup> Prompted by the recent report in this journal<sup>4</sup> that the previously described malachite green RNA aptamer<sup>5</sup> (**MGA**, Figure 1) increases the quantum yield of this dye up to 2000-fold upon binding, we decided to test modular aptameric constructs combining this aptamer as a “signaling domain” with other aptamers as “recognition domains”. We now report a series of allosteric<sup>6</sup> aptamers, containing no chemical modifications and showing fluorescence changes upon binding simultaneously malachite green (**MG**) and target analytes, **ATP**, flavin mononucleotide (**FMN**), and theophylline (**TH**). **FMN** and **TH** sensors consist only of RNA and, thus, represent the proof-of-principle of expressible aptameric sensors.

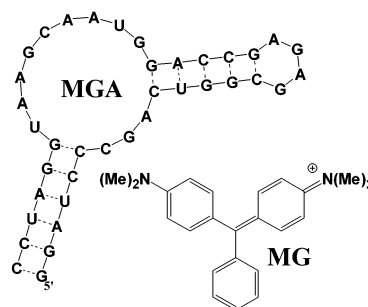


**Figure 1.** Structure of malachite green (**MG**) and malachite green aptamer (**MGA**).

Modular design has previously been applied to achieve the allosteric regulation of nucleic-acid catalysts.<sup>7</sup> While allosteric aptamers binding dyes and small molecules have been isolated through a selection-and-amplification procedure earlier,<sup>6</sup> the lack of effective readout hindered practical applications of similar systems. We have recently achieved colorimetric readout using isosteric antagonistic binding between a dye and cocaine;<sup>2b</sup> however, this system had little potential for general intracellular applications. The report by Tsien and colleagues that the free malachite green dye has only negligible fluorescence rekindled our interest in the allosteric regulation of binding events in nucleic-acid aptamers. In particular, for the first time we could test our ability to couple binding of analytes and dyes in specific and separate binding pockets, and with a concomitant analyte-dependent change in fluorescence. Up to now, and unlike with proteins, oligonucleotides that spontaneously form fluorophores have not been discovered. With the development of this new

- (1) (a) Jayasena, S. D. *Clin. Chem.* **1999**, *45*, 1628. (b) Yamamoto, R.; Kumar, P. K. R. *Gen. Cell.* **2000**, *5*, 389. (c) Jhaveri, S.; Rajendran, M.; Ellington, A. D. *Nat. Biotechnol.* **2000**, *18*, 1293–1297. (d) Jhaveri, S. D.; Kirby, R.; Conrad, R.; Maglott, E. J.; Bowser, M.; Kennedy, R. T.; Glick, G.; Ellington, A. D. *J. Am. Chem. Soc.* **2000**, *122*, 2469–2473. (e) Nutiu, R.; Li, Y. *J. Am. Chem. Soc.* **2003**, *125*, 4771–4778. (f) Ho, H. A.; Leclerc, M. *J. Am. Chem. Soc.* **2004**, *126*, 1384.
- (2) (a) Stojanovic, M. N.; Green, E. G.; Semova, S.; Landry, D. W. *J. Am. Chem. Soc.* **2003**, *125*, 6085–6089. (b) Stojanovic, M. N.; Landry, D. W. *J. Am. Chem. Soc.* **2002**, *124*, 9678–9679. (c) Stojanovic, M. N.; de Prada, P.; Landry, D. W. *J. Am. Chem. Soc.* **2000**, *122*, 11547–11548. (d) Stojanovic, M. N.; de Prada, P.; Landry, D. W. *J. Am. Chem. Soc.* **2001**, *123*, 4503–4508.
- (3) Zhang, J.; Campbell, R. E.; Ting, A. Y.; Tsien, R. Y. *Nat. Rev. Mol. Cell Biol.* **2002**, *3*, 906.
- (4) Babendure, J. R.; Adams, S. R.; Tsien, R. Y. *J. Am. Chem. Soc.* **2003**, *125*, 14716.
- (5) Grate, D.; Wilson, C. *Proc. Natl. Acad. Sci. U.S.A.* **1999**, *96*, 6131–6136.
- (6) Cholic acid competes for binding with Cibacron Blue in allosteric aptamer: Wu, L.; Curran, J. F. *Nucleic Acids Res.* **1999**, *27*, 1512.

- (7) (a) Breaker R. R. *Curr. Opin. Biotechnol.* **2002**, *13*, 31–39 and the following references therein: (b) Tang, J.; Breaker, R. R. *Nucleic Acids Res.* **1998**, *26*, 4214–4221. (c) Soukup, G.; Breaker, R. R. *Proc. Natl. Acad. Sci. U.S.A.* **1999**, *96*, 3584–3589. For the modular design of ligases: (d) Robertson, M. P.; Ellington, A. D. *Nucleic Acids Res.* **2000**, *28*, 1751–1759.

system, we could express the allosteric aptamer, add the dye to a media, and follow the formation of the fluorescent complex. Our long-term plan is to expand this ability to regulate fluorescence of the noncovalent complexes through allosteric effects to intracellular and, eventually, whole animal applications.

## Results

**Construction of Chimeric ATP Sensors.** We decided to test our idea first on a chimeric construct, combining DNA aptamer binding **ATP**<sup>8</sup> (**ATPA**) with malachite green aptamer. Our choice was the result of several considerations. First, this aptamer was successfully used in several approaches,<sup>1d,e</sup> and we could clearly compare our approach to others. Next, this aptamer is comparably short, so we could rapidly have synthetic sensors assembled on an oligonucleotide synthesizer. Finally, the DNA part of the sensor guaranteed somewhat increased stability of the construct, at least toward endonucleases.

Designwise, in an analogy to modularly designed nucleic-acid catalysts,<sup>7</sup> we expected that the typical modularly designed aptameric sensor would consist of three domains (modules): a signaling domain (malachite green aptamer), a recognition domain (analyte aptamer), and a connecting stem (communication module), which should transduce the recognition of **ATP** into an increased recognition of malachite green and concomitantly increase fluorescence. The reported malachite green aptamer has two stems onto which another aptamer could be attached through a communication module. Again, in an analogy to nucleic-acid catalysts, we decided to construct chimeras with a signaling domain at the outer portion (5' and 3' ends) of the construct. Recognition and signaling domains have conserved core structures, so we focused our engineering efforts mostly on the communication module. We were particularly interested in achieving positive regulation, because any detection of an analyte is rendered more sensitive by the low background fluorescence in the absence of an analyte. Our idea was to connect two aptamers through their double helical regions, and then weaken the common stem until we see a response, which is defined as an increase in malachite green fluorescence upon increase in **ATP** concentration. In other words, we hoped to achieve the situation in which the binding of **ATP** would stabilize the formation of **MG** aptamer.

Initially, we constructed five chimeric constructs (Figure 2) and tested them for fluorescence in the presence of 1  $\mu\text{M}$  **MG** and in the buffer mimicking intracellular milieu (20 mM TRIS, pH = 7.4, 140 mM KCl, 5 mM NaCl, 5 mM  $\text{MgCl}_2$ ) in the presence and absence of 1 mM **ATP**. These chimeric candidates were constructed to address the influence of not only the communication stem, but also of an outer stem of the **MGA**. In general, what we observed is what could be explained by straightforward reasoning: (1) increased lengths of both outer and communication stems stabilized fluorescent complex formation, observed through an increase of fluorescence with and without **ATP** (**MGA-ATPA.5**), (2) decreased stability of the outer stem yielded a greater difference in fluorescence with and without **ATP** (cf. **MGA-ATPA.1** and **MGA-ATPA.2**), presumably because of the increased significance of the stabilization of communication stem; at the same time, (3) mismatches close to the **ATP** binding sites (GA to GT mismatch, **MGA-ATPA.4**)

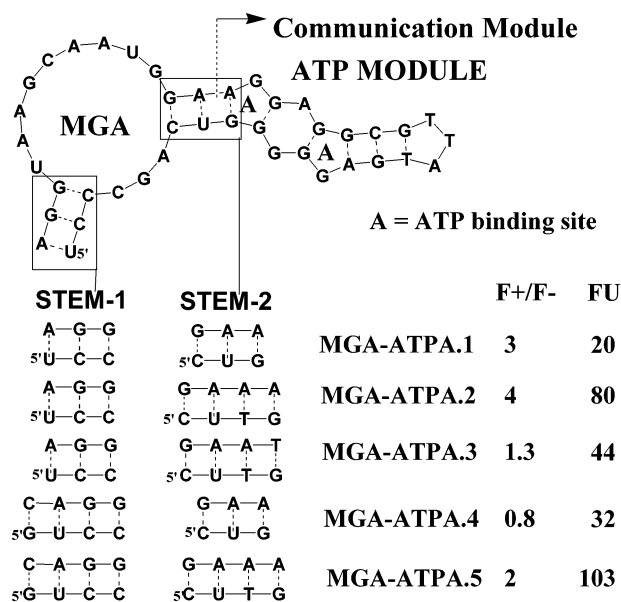


**Figure 2.** Structures of seven sensors tested, with the results of the initial screening (F+/F- ratio of fluorescence intensities in the presence and absence of 1 mM **ATP**; FU absolute value of fluorescence intensity in the presence of **ATP** in relative fluorescence units).

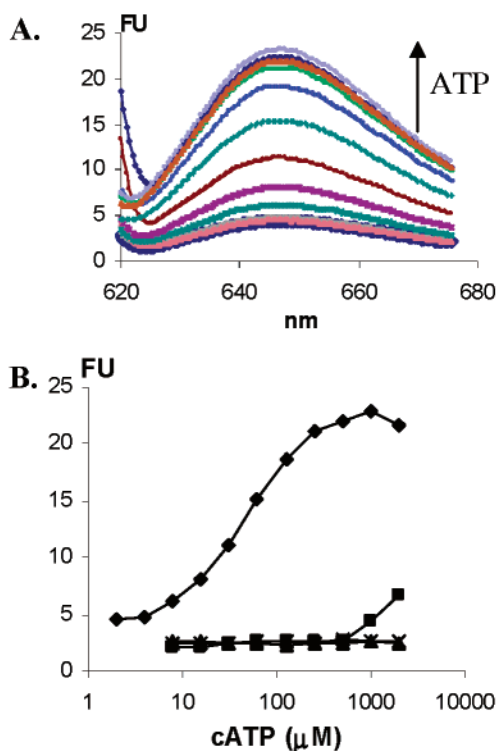


**Figure 3.** (A) Fluorescence spectra of **MGA-ATPA.1** in the presence of increasing amounts of **ATP** (from 2 mM serial dilutions, and no **ATP**, deep blue colored spectra). (B) The matching fluorescence intensity (relative units FU) of **MGA-ATPA.1** (1  $\mu\text{M}$ ) in the presence of **MG** (0.5  $\mu\text{M}$ ) and increasing concentrations of **ATP** ( $\blacklozenge$ ), **UTP** ( $\blacksquare$ ), **CTP** ( $\blacktriangle$ ), and **GTP** ( $\times$ ). Each spectrum and data point represent the average of three consecutive scans.

diminish signaling. For further characterization, we have chosen sensor **MGA-ATPA.1**, which showed both good response (almost a 3-fold increase), reasonable final fluorescence intensity, and low background in the absence of **ATP** (Figure 3A).

**Characterization of MGA-ATPA.1 Sensor.** We first characterized the sensor over a full range of concentrations of **ATP**,

(8) Huizenga, D. A.; Szostak, J. W. *Biochemistry* **1995**, *34*, 656.

and for the selectivity over other NTP's. In a buffer mimicking intracellular milieu, with 1  $\mu\text{M}$  sensor and 0.5  $\mu\text{M}$  MG, the sensor responded over the range of 10  $\mu\text{M}$  to 2 mM of ATP (Figure 3A), with half-saturation ( $K_d$  apparent) at approximately 50  $\mu\text{M}$  ATP, which is similar to other sensors based on this ATP aptamer.<sup>1c,e,2d</sup> The response was almost 5-fold above the background at the highest ATP concentrations, which is better than previously reported single-molecule constructs,<sup>1c</sup> but less than the best heteromeric sensors<sup>1e</sup> ("structure switching sensors"). This robustness of response is a promising characteristic for planned intracellular applications. An important distinction with previous sensors is that this construct does not require the covalent attachment of fluorophore for the sensor function. The selectivity of sensor closely followed the reported selectivity of the original aptamer.<sup>9</sup> Specifically, no response was observed with GTP and CTP, and only minimal response at the highest concentrations was observed with UTP (Figure 3B).

To further characterize the MGA-ATPA.1, we attempted to saturate it (at 1  $\mu\text{M}$ ) with an excess of MG. However, at concentrations above 10  $\mu\text{M}$  MG, fluorescence started decreasing, presumably due to nonspecific interactions between the dye and the nucleic acid, possibly causing self-quenching. On the basis of comparison with the original aptamer (MGA), under the same conditions, we estimated that below 20% of the sensor is bound to malachite green at 10  $\mu\text{M}$  MG. This indicates that  $K_d$  of the malachite green domain is around 40  $\mu\text{M}$ . After the addition of the saturating concentrations of ATP, increased complex formation to about 40% was observed, indicating that in the presence of the fully formed ATP binding pocket, the  $K_d$  of malachite green module drops to approximately 15  $\mu\text{M}$ .<sup>9</sup> These results support our proposed mechanism of allosteric regulation of the binding strength of the signaling module by the recognition module.

**Theophylline and FMN Sensors.** To demonstrate that our approach can be applied to the construction of other sensors for small molecules, we tested this design on two more analytes, theophylline (TH) and flavine mononucleotide (FMN).

The theophylline aptamer (THA)<sup>10</sup> is unique for its ability to distinguish theophylline from the closely related caffeine with selectivity greater than any of the existing anti-theophylline antibodies ( $10^4$ ). We were intrigued whether a modular sensor would be able to reproduce the exquisite selectivity of the parent aptamer. Accordingly, we constructed a theophylline sensor combining the malachite green aptamer with the theophylline aptamer through two Watson–Crick base pairs long stem to obtain MGA-THA, similar to the one used to construct the MGA-ATPA.1 sensor. As expected, this construct, in the presence of 2  $\mu\text{M}$  MG, behaved as a sensor of theophylline with an up to 8-fold increase in fluorescence intensity over the TH range from 2 to 250 nM. Importantly, MGA-THA was completely insensitive to caffeine (Figure 4B), which was in agreement with the supposition that aptamer-derived sensors conserve selectivities of their parent aptamers. Experiments similar to those performed for the MGA-ATPA.1 indicate that at the maximum concentration of MG (10  $\mu\text{M}$ ) using 1  $\mu\text{M}$

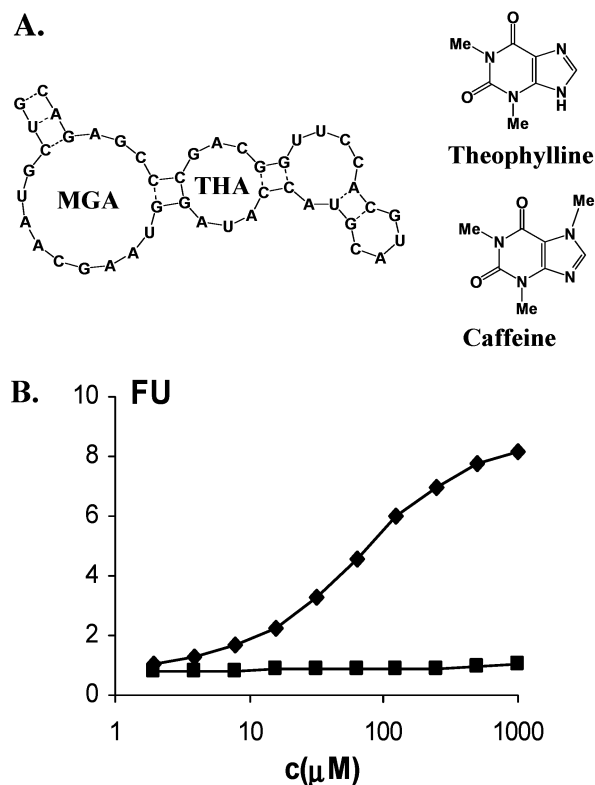


**Figure 4.** (A) Structures of theophylline sensor (MGA-THA). (B) Fluorescence intensity versus concentration curves for theophylline ( $\blacklozenge$ ) and caffeine ( $\blacksquare$ ). Each spectrum and data point represent the average of three consecutive scans (MGA-THA 1  $\mu\text{M}$ , MGA 2  $\mu\text{M}$ ).

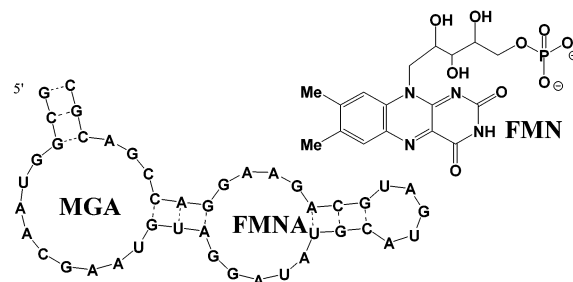


**Figure 5.** Structure of FMN sensor (MGA-FMNA) and FMN.

aptamer, approximately 3% and 20% of signaling domains are formed in the absence of theophylline and in the presence of 1 mM theophylline, respectively, indicating a change in  $K_d$  for the signaling domain from approximately 300 to 40  $\mu\text{M}$  with the TH binding.

In our final construct, the FMN sensor MGA-FMNA (Figure 5), we decided to take the communication module reported to work for the catalyst switch.<sup>7</sup> Coincidentally, this module has again only two stable Watson–Crick base pairs.<sup>11</sup> While there was no a priori reason to assume that the mechanistic basis for the successful design of the catalytic nucleic acids would be translated into the success of the modular aptameric design, we were gratified to find out that the construct (Figure 6) behaved as a sensor, with a 30–50-fold increase in fluorescence (or in binding of malachite green) at saturating concentrations of FMN. This impressive increase is based on the almost complete lack of binding to MG in the absence of theophylline, resulting in

(9) A similar  $K_d$  change was confirmed by observing an approximately 3-fold shift in the concentration of aptamer–fluorescence signal curves for the increasing concentrations of sensor in the presence of saturating concentrations of ATP (2 mM) and in the absence of analyte with MG at 330 nM. Please see the Supporting Information.

(10) Jenison, R. D.; Gill, C.; Pardi, A.; Polisky, B. *Science* **1994**, *263*, 1425–1429.

(11) The communication modules in modular nucleic-acid catalysts could have various lengths, and the switching mechanisms may be different.

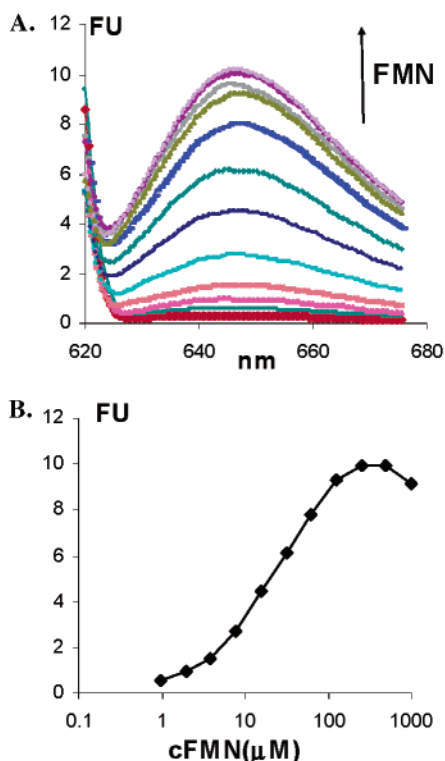


**Figure 6.** (A) Fluorescence spectra increase of MGA-FMNA ( $1 \mu\text{M}$ ) in the presence of MG ( $0.5 \mu\text{M}$ ) and increasing concentrations of FMN (background fluorescence is labeled red). (B) The matching fluorescence intensity (relative fluorescence units) versus concentration curves for flavin. Each spectrum and data point represent the average of three consecutive scans.

the low background fluorescence. The MGA-FMNA aptameric sensor, to the best of our knowledge, has the most robust signal of all reported aptameric sensors in the peer-reviewed literature. Using maximum concentrations of malachite green, the sensor is less than 1.5% bound to the dye, indicating a  $>750 \mu\text{M}$   $K_d$ . The addition of FMN causes around 15% of the signaling module to form a complex, and the  $K_d$  shifted to approximately  $30 \mu\text{M}$ . Importantly, omission of the aptamer yielded an essentially nonfluorescent solution.

## Discussion

In this work, we constructed modular allosteric fluorescent sensors without covalently attached fluorophores, and these sensors were capable of signaling the presence of small molecules. The initial concept behind these sensors was straightforward: we connected two aptamers, one binding malachite green fluorophore and another binding an analyte, through a labile connecting stem. Through this design, we targeted the mechanism of signaling (we propose to call this mechanism “cascaded stabilization”), in which the binding of an analyte to its module stabilizes the otherwise unstable connecting stem, and the formation of this stem in turn stabilizes binding of a fluorophore to the signaling module. Our proposed mechanism seems correct for all three of our sensors (MGA-ATP.1, MGA-THA, and MGA-FMNA), although we cannot exclude more complex conformational switching as a part of our mechanism. Thus, with some limitations discussed below, we should be able now to construct sensors to almost any analyte.

There are several aspects of our current sensors that leave room for further optimization and improvement: While all sensors show good and sufficient response for intracellular applications, only the MGA-FMNA sensor shows impressive signaling, stronger than any of the other previously reported aptameric sensors. Such strong response would be difficult to predict, or to design rationally and without prohibitively expensive trial-and-error approach; thus, achieving such a robust signaling is probably best accomplished with the selection and amplification process analogous to the process used to isolate the first allosteric aptamers.<sup>6</sup>

The second aspect that would be critical for widespread practical, that is, intracellular, applications is the choice of chromophore. Whether malachite green is the best choice for intracellular signaling remains an open question, at least until details of the first mRNA intracellular tracking experiments using MG are published by Tsien’s group. Malachite green generates very efficiently singlet oxygen upon irradiation. This property was previously used to achieve targeted damage of mRNA constructs<sup>5</sup> and may lead to the undesired behavior of cells during the imaging process and severe limitations in experimental setups. For example, even in vitro, we noticed that irradiation leads to the reduction of fluorescent signal, and we attributed this property to the photodestruction of RNA. Fortunately, other dyes with potentially different photooxidation properties are also available for use in these constructs.<sup>4</sup> We also note that our results with covalently attached fluorescein,<sup>2a</sup> together with earlier observations by Ellington’s group,<sup>1c</sup> indicate that the construction of the binding pocket for fluorescein could lead to significant quenching in the bound state and robust signaling (for example, up to a 4-fold increase in signal was observed in some of the sensors based on three-way junctions used in cross-reactive arrays). Finally, we note that it would be desirable to construct ratiometric sensors based on aptamers to provide internal control in the quantitative assessment of changes in the analyte concentrations.

One limitation in the rational modular design approach to sensors, described in this paper, is that some of the aptamers with preformed binding conformations lacking appropriate stems may be more difficult to use as recognition domains for the positively regulated allosteric sensors. For example, we were not able to achieve positive allosteric regulation by thrombin using reported G-quartet-based aptamer,<sup>12</sup> despite several tested chimeric constructs.<sup>13</sup> Also, we were not able to achieve an increase in fluorescence for the ATP aptamer that was previously reported to undergo steric clash with the ribozyme domain in the allosterically regulated nucleic-acid catalysts. Again, a selection process (that is, a nonrational, combinatorial process) could be used to rectify this weakness in rational approach, and we will describe our advances in this area in due course.

## Conclusions

Through our previous work, we have expanded the principles of modular design<sup>7</sup> to the molecular computation area.<sup>14</sup> Our successful construction of aptameric modular sensors expands

(12) Bock, L. C.; Griffin, L. C.; Latham, J. A.; Vermaas, E. H.; Toole, J. J. *Nature* **1992**, *355*, 564–566.

(13) However, we were able to use the steric bulk of the protein to achieve what we presume is negative steric regulation and release of malachite green: Stojanovic, M. N. *J. Serb. Chem. Soc.*, manuscript in preparation.

(14) Stojanovic, M. N.; Mitchell, T. E.; Stefanovic, D. *J. Am. Chem. Soc.* **2002**, *124*, 123–125.

the principles of modular design to yet another area, providing a new venue for the construction of molecular sensors. The robustness of responses and the fact that some of our sensors are made only of natural RNA components indicate that similar constructs have potential for applications in intracellular imaging.

### Materials and Methods

**Materials.** Oligonucleotides were custom-made and DNA/RNase free HPLC purified by Integrated DNA Technologies, Inc. (Coralville, IA) or TriLink Biotechnologies (San Diego, CA) and were used as received. DNase/RNase free water was purchased from ICN (Costa Mesa, CA) and used for all buffers, and for stock solutions of sensors, which were made at 100  $\mu$ M. NTP stock solutions (100 mM) were purchased from Promega (Madison, WI); malachite green, theophylline, caffeine, and FMN were purchased from Sigma-Aldrich Co. (Milwaukee, WI). Binding buffer approximately mimicking intracellular milieu was used for all experiments (20 mM Tris, pH = 7.4, 5 mM MgCl<sub>2</sub>, 140 mM KCl, 5 mM NaCl).

**Instrumental.** Fluorescent spectra were taken on a Perkin-Elmer (San Jose, CA) LS-55 luminometer with a Hamamatsu Xenon lamp. Experiments were performed at the excitation wavelength of 610 nm and emission scan of 620–700 nm. The spectra were exported to Microsoft Excel files and colored appropriately.

**Characterization of MGA-ATPA.1 and MGA-FMNA.** Sensors were diluted in binding buffer to 1  $\mu$ M concentration, and malachite green (1 mM stock solution in water) was added at desired concentrations (e.g., in the experiments for Figure 1, 0.5  $\mu$ M). Series of standard dilutions of analytes (ATP, CTP, UTP, GTP, 100 mM stock, FMN, 52 mM stock) were performed in sensor solution, and three fluorescent readings were taken with each solution within 5 min.

**Characterization of MGA-THA.** Sensor was diluted in binding buffer to 1  $\mu$ M concentration, and malachite green was added to 2  $\mu$ M. To avoid dilution in the first samples (due to low solubility of

theophylline and caffeine and a diluted stock solution of 1 mM), 2-fold serial dilutions were performed in buffer, and sensor solution was added afterward.

**Estimations of K<sub>d</sub>'s.** Sensor was diluted in binding buffer to 1  $\mu$ M concentration, and malachite green was added to 10  $\mu$ M. The fluorescence intensity of this sample was compared to the fluorescence intensity of the MGA aptamer under the same conditions. This was used to estimate the % formed complex in the absence of ligand (calculated as the ratio of fluorescence intensities between solutions of sensors, and MGA solution), % free aptamer (nonfluorescent species, calculated on the basis of the complex formation extent), and the concentration of malachite green (nonfluorescent species, in most of the cases assumed unchanged, due to the large excess of dye). These values were used directly in the equation for K<sub>d</sub> to estimate its value. Exactly the same experiment was performed in the presence of the saturating concentrations of individual ligands.

**Acknowledgment.** Our sensor work is supported by the NIH (NIBIB, RO1 EB000675) and the NSF (Biophotonics Grant, BES-0321972). Our work on the recognition-triggered small molecule release (and binding) is funded by NASA (NAS2-02039). M.N.S. is particularly grateful for the support from the Searle Scholars Program.

**Supporting Information Available:** (1) Fluorescence values for experiments performed in the presence of 10  $\mu$ M MG: (a) for ATP; (b) for theophylline; (c) for FMN. (2) Saturation of fluorescence in the presence of 10  $\mu$ M MG exemplified on 1  $\mu$ M MGA-THA sensor. (3) Concentration of aptamer–fluorescence signal curves for increasing concentrations of aptamer in the presence of 330 nM MG and in the presence and absence of 1 mM ATP. This material is available free of charge via the Internet at <http://pubs.acs.org>.

JA032013T